

Dynamic flight stability of hovering insects

Mao Sun · Jikang Wang · Yan Xiong

Received: 12 September 2006 / Revised: 13 December 2006 / Accepted: 5 January 2007 / Published online: 22 May 2007
© Springer-Verlag 2007

Abstract The equations of motion of an insect with flapping wings are derived and then simplified to that of a flying body using the “rigid body” assumption. On the basis of the simplified equations of motion, the longitudinal dynamic flight stability of four insects (hoverfly, crane fly, drone fly and hawkmoth) in hovering flight is studied (the mass of the insects ranging from 11 to 1,648 mg and wingbeat frequency from 26 to 157 Hz). The method of computational fluid dynamics is used to compute the aerodynamic derivatives and the techniques of eigenvalue and eigenvector analysis are used to solve the equations of motion. The validity of the “rigid body” assumption is tested and how differences in size and wing kinematics influence the applicability of the “rigid body” assumption is investigated. The primary findings are: (1) For insects considered in the present study and those with relatively high wingbeat frequency (hoverfly, drone fly and bumblebee), the “rigid body” assumption is reasonable, and for those with relatively low wingbeat frequency (crane fly and hawkmoth), the applicability of the “rigid body” assumption is questionable. (2) The same three natural modes of motion as those reported recently for a bumblebee are identified, i.e., one unstable oscillatory mode, one stable fast subsidence mode and one stable slow subsidence mode. (3) Approximate analytical expressions of the eigenvalues, which give physical insight into the genesis of the natural modes of motion, are derived. The expressions identify the speed derivative M_u (pitching moment produced by unit horizontal speed) as the primary source

of the unstable oscillatory mode and the stable fast subsidence mode and Z_w (vertical force produced by unit vertical speed) as the primary source of the stable slow subsidence mode.

Keywords Insect · Dynamic stability · Equations of motion · Navier–Stokes simulation · Natural modes of motion

1 Introduction

Considerable progress has been made in the area of aerodynamics of insect flight in the last 20 years [1–3]. With the current understanding of the aerodynamic force mechanisms of insect flapping wings, researchers are beginning to study the dynamics of insect flight. Thomas and Taylor [4] and Taylor and Thomas [5] studied static stability of gliding animals and flapping flight, respectively, and they found that flapping did not have any inherently destabilizing effect, and that flapping could even enhance static stability compared to gliding flight at a given speed.

Taylor and Thomas [6] and Sun and Xiong [7] studied dynamic flight stability in the desert locust at forward flight and in a bumblebee at hovering flight, respectively. An important assumption, “rigid body” assumption, was made in their analysis. With this assumption, the analysis was greatly simplified. The “rigid body” assumption is that the insect had only 6 degrees of freedom of a rigid flying body and the effects of the flapping wings on the flight system are represented by wingbeat-cycle-average aerodynamic and inertial forces and moments that can vary with time over the time scale of the insect body. It is further assumed that the animal’s motion consists of small disturbances from the equilibrium condition; thus, the linear theory of aircraft flight dynamics is applicable to the analysis of insect flight dynamics.

The project supported by the National Natural Science Foundation of China (10232010 and 10472008).

M. Sun (✉) · J. Wang · Y. Xiong
Institute of Fluid Mechanics, Beihang University,
Beijing 100083, China
e-mail: m.sun@263.net

The equations of motion of a body of 6 degrees of freedom were directly used under the “rigid body” assumption. The authors did not first develop the full equations of motion of an insect (body plus the flapping wings) and then simplify the equations to that of a body. As a result, the simplification process could not be examined and its validity could not be tested. In the present study, we first derive the full equations of motion of an insect with flapping wings; and then we reduce the equations of motion to that of a body with 6 degree of freedom using the “rigid body” assumption. By doing so, the simplification process can be examined and the magnitudes of the neglected terms can be estimated.

Different insects have very different sizes and wingbeat frequencies, it is of great interest to investigate the size and wing kinematics influence on the validity of the “rigid body” assumption. In the present study, we address this question by studying the longitudinal dynamic stability in hovering flight of four insects (a hoverfly, a dronefly, a crane fly, and a hawkmoth; their mass ranging from 11 to 1,648 mg and wingbeat frequency ranging from 26 to 157 Hz). These insects are chosen because their sizes and wingbeat frequencies are different greatly, and because their morphological and wing kinematic data are available from previous studies.

In the study of Sun and Xiong [7], numerical solutions for the eigenvalues were obtained. The solutions, although they could show the properties of the natural modes of motion, do not give much physical insight into their genesis. If approximate analytical solutions are obtained, the production of the natural modes of motion and the influence of the flight parameters could be better understood. In the present study, approximate analytical expressions of the eigenvalues are derived and physical insight into the genesis of the natural modes of motion can be obtained.

Similar to Ref. [7], we use the method of Computation Fluid Dynamics (CFD) to compute the flows and to obtain the aerodynamic derivatives and use the techniques of eigenvalue and eigenvector analysis to study the properties of the dynamic flight stability of the hovering insects.

2 The model of analysis and the solution methods

2.1 Equations of motion and fluid dynamics equations

Equations of motion for flapping flight have been developed and presented by Gebert et al. [8]. However, due to some errors, their equations cannot be used as they are. We have re-derived the equations in Appendix A. Three frames of reference are used, as seen in Fig. 1: frame (x_f, y_f, z_f) is an inertial frame; frame (x_b, y_b, z_b) is a frame fixed on the insect body with its origin at the centre of gravity of the wingless

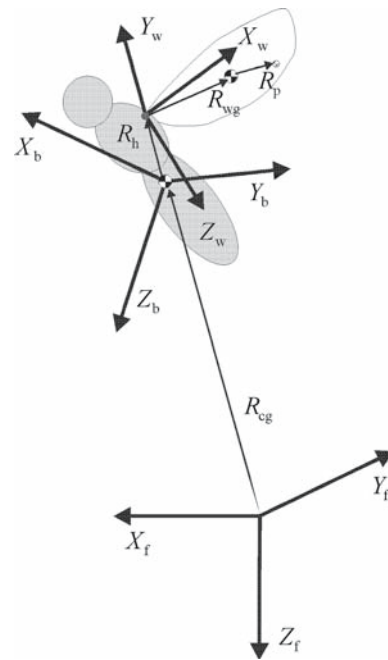


Fig. 1 Reference frames

body; frame (x_w, y_w, z_w) is a frame fixed on an insect wing with its origin at the root of the wing. For any vector V , in frame (x_f, y_f, z_f) we have:

$${}_fV = \begin{bmatrix} Vx_f \\ Vy_f \\ Vz_f \end{bmatrix}, \tag{1}$$

where Vx_f , Vy_f and Vz_f are the x_f , y_f and z_f components of V , respectively. Similarly, in frame (x_b, y_b, z_b) and frame (x_w, y_w, z_w) , we have, respectively:

$${}_bV = \begin{bmatrix} Vx_b \\ Vy_b \\ Vz_b \end{bmatrix} \tag{2}$$

and ${}_wV = \begin{bmatrix} Vx_w \\ Vy_w \\ Vz_w \end{bmatrix}$.

${}_fV$, ${}_bV$ and ${}_wV$ are related by the following relations [9].

$$\begin{aligned} {}_fV &= \mathbf{E}_{b \rightarrow f} {}_bV, \\ {}_fV &= \mathbf{E}_{w \rightarrow f} {}_wV, \\ \text{and } {}_bV &= \mathbf{E}_{w \rightarrow b} {}_wV. \end{aligned} \tag{3}$$

Here $\mathbf{E}_{b \rightarrow f}$, $\mathbf{E}_{w \rightarrow f}$ and $\mathbf{E}_{w \rightarrow b}$ are matrix of direction cosines. For example,

$${}_{b \rightarrow f} \mathbf{E} = \begin{bmatrix} \cos \theta \cos \psi & \sin \phi \sin \theta \cos \psi - \cos \phi \sin \psi & \cos \phi \sin \theta \cos \psi + \sin \phi \sin \psi \\ \cos \theta \sin \psi & \sin \phi \sin \theta \sin \psi + \cos \phi \cos \psi & \cos \phi \sin \theta \sin \psi - \sin \phi \cos \psi \\ -\sin \theta & \sin \phi \cos \theta & \cos \phi \cos \theta \end{bmatrix}, \tag{4}$$

where ψ , θ and ϕ are the Euler angles relating frame (x_b, y_b, z_b) to frame (x_f, y_f, z_f) ;

$${}_{w \rightarrow b} \mathbf{E} = \begin{bmatrix} \cos \theta_w \cos \psi_w & \sin \phi_w \sin \theta_w \cos \psi_w - \cos \phi_w \sin \psi_w & \cos \phi_w \sin \theta_w \cos \psi_w + \sin \phi_w \sin \psi_w \\ \cos \theta_w \sin \psi_w & \sin \phi_w \sin \theta_w \sin \psi_w + \cos \phi_w \cos \psi_w & \cos \phi_w \sin \theta_w \sin \psi_w - \sin \phi_w \cos \psi_w \\ -\sin \theta_w & \sin \phi_w \cos \theta_w & \cos \phi_w \cos \theta_w \end{bmatrix}, \tag{5}$$

where ψ_w , θ_w and ϕ_w are the Euler angles relating frame (x_w, y_w, z_w) to frame (x_b, y_b, z_b) . With respect to the inertial frame, the centre of gravity of the wingless body moves at velocity \mathbf{v}_{cg} , the body rotates at angular velocity $\boldsymbol{\omega}_{bd}$ and a wing rotates at angular velocity $\boldsymbol{\omega}_{wg}$ (note that since angular velocity of the wing relative to the body is prescribed, $\boldsymbol{\omega}_{wg}$ and $\boldsymbol{\omega}_{bd}$ are not independent). \mathbf{R}_{cg} is the position vector of the centre of gravity of the body; \mathbf{R}_h is the vector from the body centre of gravity to the root of a wing; \mathbf{R}_{wg} is the vector from the root of a wing to the centre of gravity of the wing; \mathbf{R}_p is the vector from the centre of gravity of a wing to any point on the wing (Fig. 1).

Let \mathbf{F}_A be the total aerodynamic force and \mathbf{M}_A moment (about the centre of gravity of the body), m_{total} the total mass of the insect (body and wings), m_{wg} the mass of a wing, \mathbf{I}_b the matrix of moments and products of inertia of the body, \mathbf{I}_{wg} the matrix of moments and products of inertia of a wing, \mathbf{g} the gravitational acceleration and t the time. The equations of motion (Eqs. A14 and A39 in Appendix A) are as follows:

$$\begin{aligned} & {}_b \mathbf{F}_A + \left[m_{bd} + \sum_{i=1}^N m_{wg,i} \right] \mathbf{b} \mathbf{g} \\ &= \left[m_{bd} + \sum_{i=1}^N m_{wg,i} \right] \left(\frac{d_b \mathbf{v}_{cg}}{dt} + {}_b \boldsymbol{\omega}_{bd} \times {}_b \mathbf{v}_{cg} \right) \\ &+ \sum_{i=1}^N \left\{ m_{wg} \left[\frac{d_b \boldsymbol{\omega}_{bd}}{dt} \times {}_b \mathbf{R}_h + {}_b \boldsymbol{\omega}_{bd} \times ({}_b \boldsymbol{\omega}_{bd} \times {}_b \mathbf{R}_h) \right] \right\}_i \\ &+ \sum_{i=1}^N \left\{ m_{wg} {}_w \mathbf{E} \left[\frac{d_w \boldsymbol{\omega}_{wg}}{dt} \times {}_w \mathbf{R}_{wg} \right. \right. \\ &\left. \left. + {}_w \boldsymbol{\omega}_{wg} \times ({}_w \boldsymbol{\omega}_{wg} \times {}_w \mathbf{R}_{wg}) \right] \right\}_i, \tag{6} \\ & {}_b \mathbf{M}_A + \sum_{i=1}^N [m_{wg} ({}_b \mathbf{R}_h + {}_b \mathbf{R}_{wg}) \times \mathbf{b} \mathbf{g}]_i \\ &= {}_b \boldsymbol{\omega}_{bd} \times {}_b \mathbf{I}_{bdb} \boldsymbol{\omega}_{bd} + \frac{d}{dt} \left\{ {}_b \mathbf{I}_{bdb} \boldsymbol{\omega}_{bd} \right. \end{aligned}$$

$$\begin{aligned} & \left. + \sum_{i=1}^N [m_{wg} ({}_b \mathbf{R}_h + {}_b \mathbf{R}_{wg}) ({}_b \mathbf{v}_{cg} + {}_b \boldsymbol{\omega}_{bd} \times {}_b \mathbf{R}_h) \right. \\ & \left. + m_{wg} {}_b \mathbf{R}_h \times ({}_b \boldsymbol{\omega}_{wg} \times {}_b \mathbf{R}_{wg}) + {}_w \mathbf{E} ({}_w \mathbf{I}_{wgw} \boldsymbol{\omega}_{wg}) \right]_i \\ & + \sum_{i=1}^N \left\{ {}_b \boldsymbol{\omega}_{bd} \times {}_w \mathbf{E} ({}_w \mathbf{I}_{wgw} \boldsymbol{\omega}_{wg}) + m_{wg} {}_b \boldsymbol{\omega}_{bd} \right. \\ & \times [{}_b \mathbf{R}_h \times ({}_b \boldsymbol{\omega}_{wg} \times {}_b \mathbf{R}_{wg})] + m_{wg} {}_b \boldsymbol{\omega}_{bd} \times [({}_b \mathbf{R}_h + {}_b \mathbf{R}_{wg}) \\ & \times ({}_b \mathbf{v}_{cg} + {}_b \boldsymbol{\omega}_{bd} \times {}_b \mathbf{R}_h)] + m_{wg} {}_b \mathbf{v}_{cg} \times ({}_b \boldsymbol{\omega}_{bd} \times {}_b \mathbf{R}_h \\ & \left. + {}_b \boldsymbol{\omega}_{wg} \times {}_b \mathbf{R}_{wg}) \right\}_i, \tag{7} \end{aligned}$$

where N is the number of wings, and ${}_b \mathbf{F}$, ${}_b \mathbf{M}$ and m_{total} in Eqs. (A14) and (A39) have been replaced by ${}_b \mathbf{F} = {}_b \mathbf{F}_A + [m_{bd} + \sum_{i=1}^N m_{wg,i}] \mathbf{b} \mathbf{g}$, ${}_b \mathbf{M} = {}_b \mathbf{M}_A + \sum_{i=1}^N [m_{wg} ({}_b \mathbf{R}_h + {}_b \mathbf{R}_{wg}) \times \mathbf{b} \mathbf{g}]_i$ and $m_{total} = [m_{bd} + \sum_{i=1}^N m_{wg,i}]$, where m_{bd} is the mass of the body.

The aerodynamic force and moment (\mathbf{F}_A and \mathbf{M}_A in Eqs. (6) and (7)) are determined by fluid dynamic equations (the Navier–Stokes equations). The equations can be found in Ref. [3] and will not be repeated here.

2.2 Simplification of the equations of motion by “rigid body” assumption

The motion of the insect is governed by the two systems of equations, the system of equations of motion and the system of fluid dynamics equations. These equations are very complex. With “rigid body” assumption, the equations of motion can be greatly simplified, and furthermore, flight stability of an insect can be made similar to that of aircraft.

We first re-write Eqs. (6) and (7) as follows. Let $\boldsymbol{\omega}_{wg0}$ represent the angular velocity of the wing relative to the body, which is determined by the flapping motion of the wing, then $\boldsymbol{\omega}_{wg}$ can be written as

$${}_w \boldsymbol{\omega}_{wg} = {}_w \boldsymbol{\omega}_{wg0} + {}_w \mathbf{E} {}_b \boldsymbol{\omega}_{bd}, \tag{8}$$

$${}_b \boldsymbol{\omega}_{wg} = {}_w \mathbf{E} {}_w \boldsymbol{\omega}_{wg} = {}_b \boldsymbol{\omega}_{wg0} + {}_b \boldsymbol{\omega}_{bd}. \tag{9}$$

Substituting Eqs. (8) and (9) into Eqs. (6) and (7) and after some manipulation, we have (assuming the insect with two wings):

$${}_bF_A + m_{bdb}g = m_{bd} \left(\frac{d_b v_{cg}}{dt} + {}_b\omega_{bd} \times {}_b v_{cg} \right) + a_1 + b_1, \tag{10}$$

$${}_bM_A = {}_b\omega_{bd} \times {}_bI_{bdb}\omega_{bd} + {}_bI_{bd} \frac{d_b \omega_{bd}}{dt} + a_2 + b_2 \tag{11}$$

where

$$a_1 = m_{wg} \sum_{i=1}^2 \left\{ -{}_b g + \frac{d_b v_{cg}}{dt} + {}_b\omega_{bd} \times {}_b v_{cg} + \frac{d_b \omega_{bd}}{dt} \times ({}_bR_h + {}_bR_{wg}) + {}_b\omega_{bd} \times [{}_b\omega_{bd} \times ({}_bR_h + {}_bR_{wg})] \right\}_i, \tag{12}$$

$$b_1 = m_{wg} \sum_{i=1}^2 \left\{ \left(\overset{E}{w \rightarrow b} \overset{\dot{E}}{b \rightarrow w} {}_b\omega_{bd} + \overset{E}{w \rightarrow b} \frac{d_w \omega_{wg0}}{dt} \right) \times {}_bR_{wg} + ({}_b\omega_{bd} + {}_b\omega_{wg0}) \times ({}_b\omega_{wg0} \times {}_bR_{wg}) + {}_b\omega_{wg0} \times ({}_b\omega_{bd} \times {}_bR_{wg}) \right\}_i, \tag{13}$$

$$a_2 = \sum_{i=1}^2 \left\{ m_{wg} ({}_bR_h + {}_bR_{wg}) \times \left(-{}_b g + \frac{d_b v_{cg}}{dt} + \frac{d_b \omega_{bd}}{dt} \times {}_bR_h \right) + m_{wgb}R_h \times \left(\frac{d_b \omega_{bd}}{dt} \times {}_bR_{wg} \right) + m_{wgb}v_{cg} \times [{}_b\omega_{bd} \times ({}_bR_h + {}_bR_{wg})] + m_{wgb}\omega_{bd} \times [({}_bR_h + {}_bR_{wg}) \times ({}_b v_{cg} + {}_b\omega_{bd} \times {}_bR_h)] + {}_bR_h \times ({}_b\omega_{bd} \times {}_bR_{wg}) + \overset{E}{w \rightarrow b} {}_wI_{wg} \overset{E}{b \rightarrow w} \frac{d_b \omega_{bd}}{dt} + {}_b\omega_{bd} \times \left[\overset{E}{w \rightarrow b} {}_wI_{wg} \left(\overset{E}{b \rightarrow w} {}_b\omega_{bd} \right) \right] \right\}_i, \tag{14}$$

$$b_2 = \sum_{i=1}^2 \left\{ m_{wgb}R_h \times \left[\frac{d_b \omega_{wg0}}{dt} \times {}_bR_{wg} + ({}_b\omega_{wg0} + {}_b\omega_{bd}) \times \left(\overset{\dot{E}}{w \rightarrow b} {}_wR_{wg} \right) \right] + \overset{\dot{E}}{w \rightarrow b} {}_wI_{wg} ({}_w\omega_{wg0} + \overset{E}{b \rightarrow w} {}_b\omega_{bd}) + \overset{E}{w \rightarrow b} {}_wI_{wg} \frac{d_w \omega_{wg0}}{dt} + {}_b\omega_{bd} \times \left(\overset{E}{w \rightarrow b} {}_wI_{wg} {}_w\omega_{wg0} \right) + \overset{E}{w \rightarrow b} {}_wI_{wg} \overset{\dot{E}}{b \rightarrow w} {}_b\omega_{bd} + m_{wgb}\omega_{bd} \times [{}_bR_h \times ({}_b\omega_{wg0} \times {}_bR_{wg})] + m_{wg} \left(\overset{\dot{E}}{w \rightarrow b} {}_wR_{wg} \right) \times ({}_b v_{cg} + {}_b\omega_{bd} \times {}_bR_h) + m_{wgb}v_{cg} \times ({}_b\omega_{wg0} \times {}_bR_{wg}) \right\}_i, \tag{15}$$

where the top dot “.” represents time derivative. In Eqs. (10) and (11), a_1 represents the weight of the wings, the inertial

force of the wings due to the body acceleration and rotation and a_2 represents the moments produced by the weight of the wings and by the inertial forces of the wings due to the body motion; b_1 and b_2 represent the inertial forces and moments of the wings due to the flapping motion. Without a_1 , a_2 , b_1 and b_2 , Eqs. (10) and (11) would be the equations of motion of a flying body.

Because m_{wg} is much smaller than m_b , compared with the terms of body weight ($m_{bd}g$) and body inertial force [$m_{bd}(d_b v_{cg}/dt + {}_b\omega_{bd} \times {}_b v_{cg})$], a_1 in the Eq. (10) can be neglected, and similarly a_2 in Eq. (11) can be neglected. Thus we have

$${}_bF_A + m_{bdb}g = m_{bd} \left(\frac{d_b v_{cg}}{dt} + {}_b\omega_{bd} \times {}_b v_{cg} \right) + b_1, \tag{16}$$

$${}_bM_A = {}_b\omega_{bd} \times {}_bI_{bdb}\omega_{bd} + {}_bI_{bd} \frac{d_b \omega_{bd}}{dt} + b_2. \tag{17}$$

Now, we further simplify Eqs. (16) and (17) using the “rigid body” assumption. The main point of the “rigid body” assumption is as following: the wingbeat frequency is relatively high, so that the time scale of the wingbeat motion is much smaller than that of the body motion, and when analyzing the flight dynamic of the insect, the wingbeat-cycle average aerodynamic and inertial forces and moments, which could vary over the time scale of the body, can be used. We take the time average of Eqs. (16) and (17) over the fast time scale (the wingbeat period) to average out the fast motion. The resulting equations would represent the body motion at the slow time scale. Let the over-bar denote the mean value (wingbeat-cycle average value) and the symbol “ $\hat{\cdot}$ ” denote the difference between the instantaneous and mean values (e.g., $v_{cg} = \bar{v}_{cg} + \hat{v}_{cg}$). Taking the time average of Eqs. (16) and (17) gives:

$${}_b\bar{F}_A + m_{bdb}g = m_{bd} \left(\frac{d_b \bar{v}_{cg}}{dt} + {}_b\bar{\omega}_{bd} \times {}_b\bar{v}_{cg} + \overline{{}_b\hat{\omega}_{bd} \times {}_b\hat{v}_{cg}} \right) + \bar{b}_1, \tag{18}$$

$${}_b\bar{M}_A = {}_b\bar{\omega}_{bd} \times {}_bI_{bdb}\bar{\omega}_{bd} + \overline{{}_b\hat{\omega}_{bd} \times {}_bI_{bdb}\hat{\omega}_{bd}} + {}_bI_{bd} \frac{d_b \bar{\omega}_{bd}}{dt} + \bar{b}_2. \tag{19}$$

Note that \hat{v} and $\hat{\omega}$ represent the fast oscillation of the body due to the cyclic variations of forces and moments at wingbeat frequency. Because the wingbeat frequency is assumed to be high, it is expected that the oscillation is very small (this should be checked afterwards). Thus terms like $\hat{\omega}_{bd} \times \hat{v}_{cg}$ can be neglected. \bar{b}_1 and \bar{b}_2 are the mean inertial force and moment of the wings due to the flapping motion. Since there are acceleration and deceleration of the wing within one downstroke (or upstroke) and the motion of the wing in the upstroke is opposite to that of the downstroke, it is anticipated that \bar{b}_1 and \bar{b}_2 are approximately zero (this should be

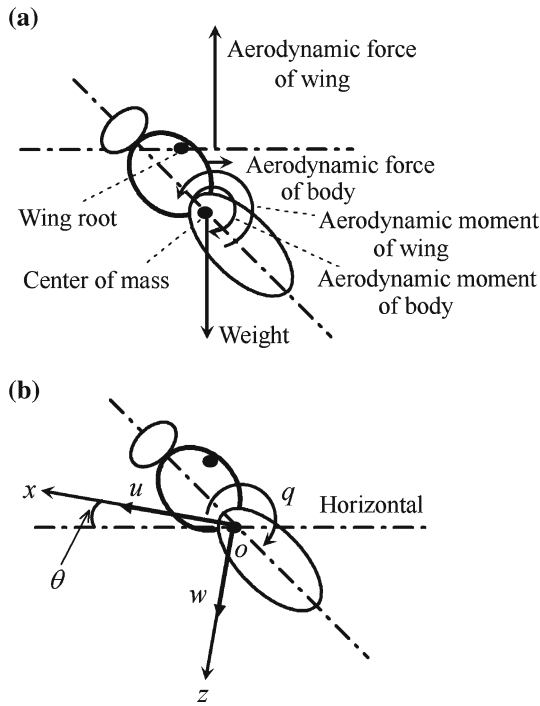


Fig. 2 **a** A sketch of the rigid body approximation. **b** Definition of the state variables

checked afterwards). As a result, Eqs. (18) and (19) become:

$${}^b\bar{F}_A + m_{bd}b\mathbf{g} = m_{bd}\left(\frac{d_b\bar{\mathbf{v}}_{cg}}{dt} + {}^b\bar{\boldsymbol{\omega}}_{bd} \times {}^b\bar{\mathbf{v}}_{cg}\right), \tag{20}$$

$${}^b\bar{M}_A = {}^b\bar{\boldsymbol{\omega}}_{bd} \times {}^bI_{bd}{}^b\bar{\boldsymbol{\omega}}_{bd} + {}^bI_{bd}\frac{d_b\bar{\boldsymbol{\omega}}_{bd}}{dt}. \tag{21}$$

Equations (20) and (21) are the simplified equations of motion (motion at the slow time scale) for the insect; they are the same as that of a rigid flying body or an airplane. (It must be emphasized that the basic assumption that the time scale of the wingbeat motion is much smaller than that of the body motion should be checked afterwards.)

2.3 Linearization of the equations of motion

Equations (20) and (21) are the same as that of an airplane; methods used in aircraft stability analysis can be used to study the stability of insects. As done to an airplane, we linearize Eqs. (20) and (21) for stability analysis. As a first step, we consider the longitudinal motion in the present study.

Let body be aligned so that the x_b -axis is horizontal and points forward at equilibrium (Fig. 2). The variables that define the motion are the forward (u) and vertical (w) components of velocity $\bar{\mathbf{v}}_{cg}$ along x_b - and z_b -axes, respectively, the pitching angular-velocity around the center of mass (q ; y_b component of $\bar{\boldsymbol{\omega}}_{bd}$), and the pitch angle between the x -axis and the horizontal (θ). Let X and Z be the components of \bar{F}_A along the x_b and z_b directions, respectively, M the y_b component of \bar{M}_A (pitching moment) and I_y the moment of

inertia of the body about y_b axis. The longitudinal component of Eqs. (20) and (21) are

$$\dot{u}^+ = -w^+q^+ + X^+/m_{bd}^+ - g^+ \sin \theta, \tag{22a}$$

$$\dot{w}^+ = -u^+q^+ + Z^+/m_{bd}^+ + g^+ \cos \theta, \tag{22b}$$

$$\dot{q}^+ = M^+/I_{y,b}^+, \tag{22c}$$

$$\dot{\theta} = q^+, \tag{22d}$$

where the variables have been non-dimensionalized using c , U and c/U as reference length, velocity and time, respectively, (c is the mean chord length of a wing; $U = 2\Phi nr_2$ is the mean flapping velocity, where r_2 is the radius of the second moment of wing area, Φ is the stroke amplitude and n is the wingbeat frequency): $X^+ = X/0.5\rho U^2 S_t$ (S_t is the area of two wings and ρ is the fluid density); $Z^+ = Z/0.5\rho U^2 S_t$; $M^+ = M/0.5\rho U^2 S_t c$; $m_{bd}^+ = m_{bd}/0.5\rho S_t c$; $t^+ = tU/c$; $g^+ = gc/U^2$ (g is the gravitational acceleration); $u^+ = u/U$; $w^+ = w/U$; $q^+ = qc/U$; $I_y^+ = I_y/0.5\rho S_t c^3$. Let each variable be expressed as the sum of the reference (equilibrium flight) value and the disturbance value:

$$\begin{aligned} u^+ &= u_e^+ + \delta u^+, & w^+ &= w_e^+ + \delta w^+, \\ q^+ &= q_e^+ + \delta q^+, & \theta &= \theta_e + \delta \theta, \end{aligned} \tag{23a}$$

$$\begin{aligned} X^+ &= X_e^+ + \delta X^+, & Z^+ &= Z_e^+ + \delta Z^+, \\ M^+ &= M_e^+ + \delta M^+, \end{aligned} \tag{23b}$$

where the subscript “e” denotes the equilibrium flight condition and the symbol “ δ ” denotes a small disturbance quantity. Note that $u_e = w_e = q_e = \theta_e = 0$ (θ_e is zero because x_b is chosen to be horizontal at equilibrium flight; q_e is zero for all constant-speed flight, including hovering; u_e and w_e are zero for hovering flight). Substituting Eq. (23a) into Eq. (22a) and neglecting second and higher order terms gives:

$$X_e^+ = 0, \tag{24a}$$

$$Z_e^+ + m_{bd}^+ g^+ = 0, \tag{24b}$$

$$M_e^+ = 0, \tag{24c}$$

and

$$\delta \dot{u}^+ = \delta X^+/m_{bd}^+ - g^+ \delta \theta, \tag{25a}$$

$$\delta \dot{w}^+ = \delta Z^+/m_{bd}^+, \tag{25b}$$

$$\delta \dot{q}^+ = \delta M^+/I_y^+, \tag{25c}$$

$$\delta \dot{\theta} = \delta q^+. \tag{25d}$$

Equations (24a) and (25a) are the equilibrium equation and the equation of disturbance motion, respectively. We further express the perturbations in the aerodynamic forces and moment as

$$\delta X^+ = X_u^+ \delta u^+ + X_w^+ \delta w^+ + X_q^+ \delta q^+, \tag{26a}$$

$$\delta Z^+ = Z_u^+ \delta u^+ + Z_w^+ \delta w^+ + Z_q^+ \delta q^+, \tag{26b}$$

$$\delta M^+ = M_u^+ \delta u^+ + M_w^+ \delta w^+ + M_q^+ \delta q^+, \tag{26c}$$

where X_u^+ , X_w^+ , etc. are the stability derivatives [9]. In Eq. (26a), terms of rate derivatives, such as $X_u^+ \delta \dot{u}$ (here \dot{u} is the time rate of change in u^+), are not included. This is consistent with the assumption that rate of body motion is very small. Substituting Eq. (26a) into Eq. (25a), the linearized equations of the disturbance motion are:

$$\begin{bmatrix} \delta \dot{u}^+ \\ \delta \dot{w}^+ \\ \delta \dot{q}^+ \\ \delta \dot{\theta} \end{bmatrix} = \mathbf{A} \begin{bmatrix} \delta u^+ \\ \delta w^+ \\ \delta q^+ \\ \delta \theta \end{bmatrix}, \tag{27}$$

where \mathbf{A} is the system matrix:

$$\mathbf{A} = \begin{bmatrix} X_u^+/m_{bd}^+ & X_w^+/m_{bd}^+ & X_q^+/m_{bd}^+ & -g^+ \\ Z_u^+/m_{bd}^+ & Z_w^+/m_{bd}^+ & Z_q^+/m_{bd}^+ & 0 \\ M_u^+/I_y^+ & M_w^+/I_y^+ & M_q^+/I_y^+ & 0 \\ 0 & 0 & 1 & 0 \end{bmatrix}. \tag{28}$$

At equilibrium flight, the wing kinematic parameters must be such that Eq. (24a) is satisfied (mean vertical force balances the weight of the insect and mean horizontal force and mean pitching moment are zero). Morphological data and most of the kinematic data at hovering flight (the equilibrium flight) for the insects considered in the present study are available from previous works [10, 11]. But there are three kinematic parameters, down- and upstroke angles of attack (α_d and α_u , respectively) and mean stroke angle ($\bar{\phi}$) are not available. As will be seen below, they can be determined using the above force and moment balance requirements. When the equilibrium conditions are determined, the stability derivatives can be calculated (see below). After the stability derivatives are calculated, the system matrix \mathbf{A} is determined and the stability properties of the insect can be analyzed.

2.4 The wing, the body and the flapping motion

In determining the equilibrium conditions of the flight, we only need to calculate the flows around the wings (at equilibrium the body does not move and it is assumed that the wings and body do not interact aerodynamically). To obtain the aerodynamic derivatives, in principle we need to compute the flows around the wings and around the body. But as discussed in Sun and Xiong [7], near hovering, the aerodynamic forces and moments of the body are negligibly small compared to those of the wings, because the relative velocity that the body sees is very small. Therefore, in estimating the aerodynamic derivatives, we still only need to compute the flows around the wings. We further assume that the contralateral wings do not interact aerodynamically. As a result,

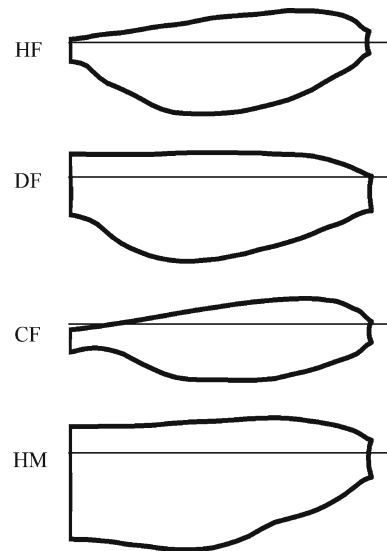


Fig. 3 The wing planforms of dronefly (DF), cranefly (CF), hawkmoth (HM)

in the present CFD model, the body is neglected and the flows around the left and right wings are computed separately. The wing planforms of the three insects (Fig. 3) are obtained from data given by Ellington [10]. The wing section is assumed to be a flat plate with rounded leading and trailing edges, the thickness of which is 3% of the mean chord length of the wing.

The flapping motion of a wing consists of two parts: the translation (azimuthal rotation) and the rotation (flip rotation). The motion is sketched in Fig. 4 (ϕ is the positional angle of the wing; ϕ_{min} and ϕ_{max} are the minimum and maximum positional angles, respectively; α is the angle of attack of the wing; β is the stroke plane angle; $o_1x_1y_1z_1$ is a frame with the x_1y_1 plane parallel to the xy plane of the body frame; $o'x'y'z'$ is a frame with the $x'y'$ plane in stroke plane). The translation (azimuthal rotation) velocity is approximated by the simple harmonic function [7]. α takes a constant value during the down- or upstroke translation (the constant value is denoted by α_d for the downstroke translation and α_u for the upstroke translation); around stroke reversal, the wing flips and α changes with time, also according to the simple harmonic function [7]. As discussed in Ref. [7], for prescribing the flapping motion, the stroke amplitude ($\Phi = \phi_{max} - \phi_{min}$), the wingbeat frequency (n), the angles of attack in the downstroke (α_d) and upstroke (α_u) translations, the mean positional angle [$\bar{\phi} = (\phi_{max} + \phi_{min})/2$] and the stroke plane angle (β) must be given.

2.5 The flow solution method

The flow equations and the solution method used are the same as those described in work by Sun and Tang [3]. The computational grids are similar to that used by Sun and Xiong

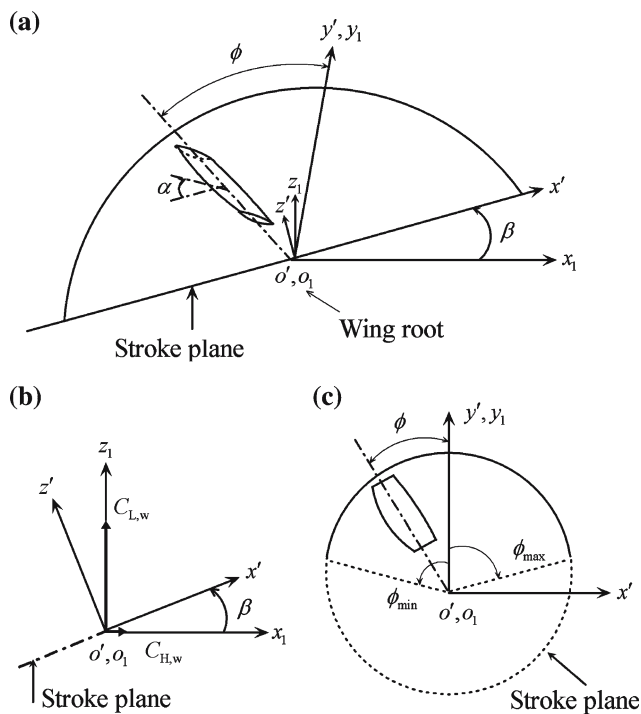


Fig. 4 Sketches of the wing motion and reference frames

[7]. Once the flow equations are numerically solved, the fluid velocity components and pressure at discretized grid points for each time step are available and the aerodynamic forces and moments acting on the wing can be calculated. Resolving resultant aerodynamic force of the wing into the z_1 - and x_1 -axis, we obtain the vertical (L_w) and the horizontal (H_w) forces due to the wing, respectively (see Fig. 3). The pitching moment about the center of mass of the insect due to the aerodynamic force on the wing is denoted as $M_{y,w}$. The above forces and moment are non-dimensionalized by $0.5\rho U^2 S$ and $0.5\rho U^2 S c$, respectively. The coefficients of L_w , H_w , and $M_{y,w}$ are denoted as $C_{L,w}$, $C_{H,w}$ and $C_{M,w}$, respectively.

2.6 Computation of the equilibrium conditions and aerodynamic derivatives

Φ , n , β of the hovering insects are available from the measured data of previous studies. The kinematics parameters of a wing left undetermined are α_d , α_u , and $\bar{\phi}$. As mentioned above, in the present study, α_d , α_u and $\bar{\phi}$ are not treated as known input parameters but are determined in the calculation process by the force balance and moment balance conditions, i.e., the mean vertical force of the wings is equal to insect weight and the mean horizontal force and mean pitching moment (about the center of mass) are equal to zero. The non-dimensional weight of an insect (C_G) is defined as $C_G = mg/0.5\rho U^2 S_t$, where $S_t = 2S$, area of two

wings. The mean vertical force coefficient of the wing needs to be equal to C_G .

Conditions in the equilibrium flight are taken as the reference conditions in the aerodynamic derivative calculations. In order to estimate the partial derivatives, X_u , X_w etc., we make three consecutive flow computations for the wing: an u -series in which u is varied whilst w , q and θ are fixed at the reference values (i.e., w , q and θ are zero), a w -series in which w is varied whilst u , q and θ are fixed at zero, and a q -series in which u , w and θ are fixed at zero (in all the three series, wing kinematical parameters are fixed at the reference values). Using the computed data, curves representing the variation of the aerodynamic forces and moments with each of the u , w and q variables are fitted. The partial derivatives are then estimated by taking the local tangent (at equilibrium) of the fitted curves.

2.7 Solution of the small disturbance equations

After the aerodynamic derivatives are determined, the elements of the system matrix A would be known. Equation (1) can be solved to yield insights into the dynamic flight stability of the hovering insects. As described in Sun and Xiong [7], the central elements of the solution for the dynamic stability problem are the eigenvalues and eigenvectors of A . A real eigenvalue and the corresponding eigenvector (or a conjugate pair of complex eigenvalues and the corresponding eigenvector pair) represent a simple motion called natural mode of motion of the system. The free motion of the flying body after an initial deviation from its reference flight is a linear combination of the natural modes of motion. A positive (or negative) real eigenvalue, λ , will result in an unstable divergent (or stable subsidence) mode; the time to double (or to half) the starting value is given by $0.693/|\lambda|$. A pair of complex conjugate eigenvalues, e.g., $\lambda_{1,2} = \hat{n} \pm \hat{\omega}i$, will result in oscillatory time variation of the disturbance quantities. The period of the oscillatory motion is $2\pi/\hat{\omega}$ and the time to double or half the oscillatory amplitude are $0.693/|\hat{n}|$.

2.8 Flight data

Flight data for the insects are taken from the works of Ellington [10,11]. The general morphological data, m , R , c , S , r_2 , l_b (body length), l_1 (distance from wing base axis to center of mass) and χ_0 (free body angle), are given in Table 1 (in the table and in the later tables and figures, HF, DF, CF and HM represent hoverfly, drone fly, crane fly and hawkmoth, respectively). Moment of inertia of the body about wing-root axis (I_b) is also available. The moment of inertia of the body about y_b -axis, can be computed as $I_y = I_b - l_1^2 m$; the computed values of I_y are also given in Table 1 (for comparison, the data of bumblebee (BB) studied in Sun and Xiong [7] are

Table 1 General morphological and wing-kinematic data for the insects

	m/mg	R/mm	c/mm	r_2/R	l_b/R	l_1/l_b	$\chi_0/(\circ)$	$I_y/(\text{kg m}^2)$	$\Phi/(\circ)$	n/Hz	$\beta/(\circ)$	$\chi/(\circ)$
HF	27.3	9.3	2.2	0.578	1.10	0.14	53	1.84×10^{-10}	90	160	0	43
DF	68.4	11.4	3.19	0.543	1.22	0.12	50	0.70×10^{-9}	109	157	0	50
CF	11.4	12.7	2.38	0.614	0.85	0.21	70	0.95×10^{-10}	120	45.5	0	51
HM	1,648	51.9	18.26	0.525	0.81	0.27	73	2.08×10^{-7}	121	26.3	0	51
BB	175	13.2	4.01	0.550	1.41	0.21	57.5	2.13×10^{-9}	116	155	6	46.8

Table 2 Parameters determined by equilibrium condition

	C_G	$\alpha_d/(\circ)$	$\alpha_u/(\circ)$	$\bar{\phi}/(\circ)$
HF	1.46	33	33	2.4
DF	1.10	5	25	0
CF	1.36	27	28	6
HM	1.51	25.5	30.5	9

also included). The available wing-kinematic data [Φ, n, β, χ (body angle)] for the insects are also given in Table 1.

3 Results and analysis

3.1 The equilibrium conditions and the aerodynamic derivatives

For different set of values of α_d, α_u and $\bar{\phi}$, the mean vertical and horizontal forces and mean pitching moment of the wings would be different. α_d, α_u and $\bar{\phi}$ are determined using the equilibrium conditions as follows. A set of values for α_d, α_u and $\bar{\phi}$ are guessed; the flow equations are solved and the corresponding mean vertical force ($\bar{C}_{L,w}$), mean horizontal force ($\bar{C}_{H,w}$) and mean moment ($\bar{C}_{M,w}$) coefficients of the wing are calculated. If $\bar{C}_{L,w}$ is not equal to C_G (the non-dimensional weight, given in Table 2), or $\bar{C}_{H,w}$ is not equal to zero, or $\bar{C}_{M,w}$ is not equal to zero, α_d, α_u and $\bar{\phi}$ are adjusted; the calculations are repeated until the magnitude of difference between $\bar{C}_{L,w}$ and C_G is less than 0.03 and those between $\bar{C}_{H,w}$ and 0 and between $\bar{C}_{M,w}$ and 0 are less than 0.01. The calculated values of α_d, α_u and $\bar{\phi}$ which satisfy the equilibrium conditions are given in Table 2.

After the equilibrium flight conditions have been determined, aerodynamic forces and moments on the wing for each of u, w and q varying independently from the equilibrium value are computed. The corresponding X^+, Z^+ and M^+ are obtained. As an example, the u -series, w -series and q -series data for the hoverfly are plotted in Fig. 5 (in the figure, the equilibrium value has been subtracted from each quantity). Similar to the case of the bumblebee studied by Sun and Xiong [7], X^+, Z^+ and M^+ vary approximately

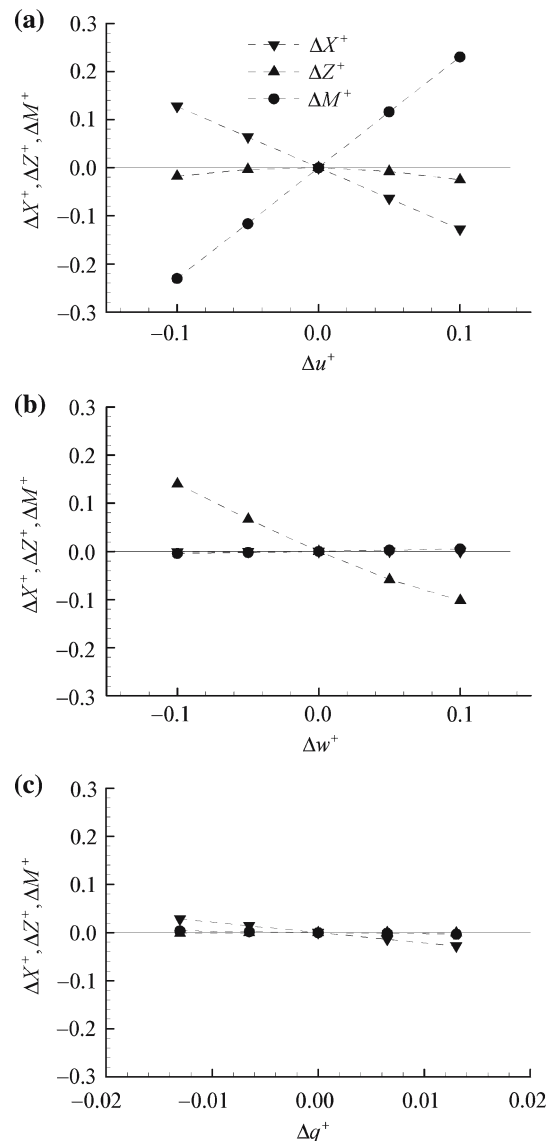


Fig. 5 The u -series (a), w -series (b) and q -series (c) force and moment data for hoverfly

linearly when the values of u^+, w^+ and q^+ are small, showing that the linearization of the equations of motion is only justified for small disturbances (results for other insects are similar).

Table 3 Non-dimensional aerodynamic derivatives

	X_u^+	Z_u^+	M_u^+	X_w^+	Z_w^+	M_w^+	X_q^+	Z_q^+	M_q^+
HF	-1.28	-0.04	2.32	0.01	-1.26	0.05	-2.15	0	-0.23
DF	-0.85	0.04	2.13	0.02	-0.99	0.04	-1.15	0.08	-0.38
CF	-1.09	-0.06	3.87	-0.01	-1.03	0.13	-1.23	0.15	-0.69
HM	-0.99	-0.12	1.97	-0.05	-1.14	0.21	-1.07	-0.08	-0.69

Table 4 Eigenvalues of the system matrix

Given in parentheses are eigenvalues non-dimensionalized by wingbeat frequency n

	Mode 1 $\lambda_{1,2}$	Mode 2 λ_3	Mode 3 λ_4
HF	0.010±0.019i (0.074±0.144i)	-0.022(-0.171)	-0.003(-0.020)
DF	0.010±0.019i (0.073±0.139i)	-0.022(-0.165)	-0.002(-0.015)
CF	0.024±0.053i (0.033±0.733i)	-0.063(-0.865)	-0.008(-0.110)
HM	0.043±0.096i (0.269±0.608i)	-0.118(-0.747)	-0.015(-0.092)
BB	0.006±0.018i (0.045±0.129i)	-0.027(-0.197)	-0.002(-0.012)

Table 5 Magnitudes and phase angles of the components of each of the three eigenvectors

Numbers in the parentheses are phase angles, in degrees

	Mode	$\delta u/U$	$\delta w/U$	$\delta qU/c$	$\delta\theta$
HF	1	1.3×10^{-1} (125)	5.0×10^{-4} (248)	0.2×10^{-1} (63)	1 (0)
	2	1.5×10^{-1} (0)	6.0×10^{-4} (0)	0.2×10^{-1} (180)	1 (0)
	3	3.0 (180)	1.4×10^2 (0)	0.3×10^{-2} (180)	1 (0)
DF	1	0.1043 (123)	0.0005 (50)	0.0213 (62)	1 (0)
	2	0.1089 (0)	0.0003 (180)	0.0223 (180)	1 (0)
	3	1.2 (180)	0.6×10^2 (0)	0.2×10^{-2} (180)	1 (0)
CF	1	0.1763 (126)	0.0018 (326)	0.0585 (66)	1 (0)
	2	0.1741 (0)	0.0039 (0)	0.0630 (180)	1 (0)
	3	5.7 (0)	1.7×10^2 (180)	0.8×10^{-2} (180)	1 (0)
HM	1	0.1803 (123)	0.0030 (231)	0.1055 (66)	1 (0)
	2	0.1730 (0)	0.0017 (0)	0.1180 (180)	1 (0)
	3	2.5 (0)	0.23×10^2 (180)	0.1×10^{-1} (180)	1 (0)

The non-dimensional aerodynamic derivatives, X_u^+ , Z_u^+ , M_u^+ , X_w^+ , Z_w^+ , M_w^+ , X_q^+ , Z_q^+ and M_q^+ are estimated using the above data and are given in Table 3. Note that although the insects have a 150-fold weight difference, each of the non-dimensional aerodynamic derivatives is not greatly different between the insects.

3.2 The natural modes of the disturbed motion

The eigenvalues and the corresponding eigenvectors, calculated in Matlab, are shown in Tables 4 and 5, respectively, (for comparison, eigenvalues for the bumblebee studied in Sun and Xiong [7] are included in Table 4). For each of the insects, there are a pair of complex eigenvalues with a positive real part and two negative real eigenvalues, representing an unstable oscillatory motion (mode 1) and

two stable subsidence motions (mode 2 and mode 3), respectively. As Sun and Xiong [7] did, we call modes 1, 2, and 3 unstable oscillatory mode, fast subsidence mode and slow subsidence mode, respectively. The three modes of motion of each of the insects are similar to the corresponding ones of the bumblebee studied by Sun and Xiong [7]. The unstable oscillatory mode is a motion in which δq , and δu are the main variables (see Table 5). In this mode the insect conducts horizontal and pitching oscillations; in a large part of a cycle, δu and δq are in phase, i.e., the insect pitching down while moving backwards or pitching up while moving forward. The fast subsidence mode is also a motion in which δq and δu are the main variables (Table 5), but δq and δu are out of phase, i.e., when δu has a positive initial value, δq has a negative initial value and the insect would pitch down (or up) back to the reference attitude and at the same time moves forward

(or backwards). The slow subsidence mode is a motion in which δw is the main variable (Table 5), which represents a vertical descending (or ascending) motion.

3.3 Test of the “rigid body” assumption

3.3.1 The requirement of body motion being much slower than wing flapping motion

The “rigid body” assumption requires that the time scale of the body motion is much larger than that of the flapping motion of the wings. The eigenvalues can determine the time scale of the body motion. If the largest eigenvalue is much smaller than the circular frequency of wingbeat, the above requirement is met.

The circular frequency of wingbeat is $2\pi n$; the non-dimensional circular frequency of wingbeat (non-dimensionalized by n) is 2π (≈ 6.28). The largest non-dimensional eigenvalue (non-dimensionalized by n) for the hoverfly, or drone fly, or bumblebee, is less than 0.2 (see Table 4), more than 30 times smaller than 2π . Thus, for these insects, the assumption should be reasonable. Note that these insects have relatively large wingbeat frequency (larger than 150 Hz; see Table 1).

However, for the crane fly or hawkmoth, the largest non-dimensional eigenvalue is about 0.8 (Table 4), only about one eighth of 2π . For these two insects, the assumption that the body motion is much slower than the wing flapping motion is in question. Note that these two insects have relatively small wingbeat frequency (25–45 Hz; see Table 1).

3.3.2 The requirement of body-oscillation at wingbeat frequency being small

In the process of simplifying the equations of motion, terms like $\hat{\omega}_{bd} \times \hat{v}_{cg}$ in Eqs. (18) and (19) have been neglected under the assumption that $\hat{\omega}_{bd}$, \hat{v}_{cg} , etc., are small, i.e., the oscillations of the body at wingbeat frequency, which is caused by cyclic variations of the aerodynamic and inertial forces on the flapping wings, are small. Here we use the complete equation of motion (Eqs. 10 and 11) to estimate the amplitude of the oscillation. Since the flapping motion (wing motion relative to the body) is prescribed, ω_{wg0} in Eqs. (10) and (11) is known. Morphological parameters such as R_h , R_{wg} , I_{wg} and so on are available or can be computed based on the data in Refs.[10,12]. As for the aerodynamic force (F_A) and moment (M_A), recall that in Sect. 3.1, the aerodynamic force and moment of the flapping wings at equilibrium flight (the body assumed not oscillating) have been computed; these force and moment are reasonably good approximations to F_A and M_A , respectively. Using these data and numerically integrating Eqs. (10) and (11), we obtain the body oscillation at equilibrium flight, which could be taken as an estimate of the body oscillation in the disturbance motion.

Table 6 The amplitude of the oscillations

	a_u/U	a_w/U	$a_q c/U$	a_θ	a_x/c	a_z/c
HF	0.013	0.0016	0.0041	0.004	0.014	0.001
DF	0.017	0.0013	0.0059	0.005	0.014	0.001
CF	0.048	0.0115	0.020	0.043	0.094	0.013
HM	0.039	0.009	0.047	0.044	0.035	0.005

The non-dimensional amplitudes of oscillation are shown in Table 6 (in the table the amplitudes of the x_b and z_b components of v_{cg} are denoted as a_u and a_w , respectively; the amplitudes of pitching angular velocity and pitching angle are denoted as a_q and a_θ , respectively; the amplitudes of the horizontal and vertical displacement of the center of mass of the body are denoted as a_x and a_z , respectively). The non-dimensional amplitudes are of the order of 10^{-2} . Thus, the magnitudes of the terms like $\hat{\omega}_{bd} \times \hat{v}_{cg}$, etc. would be of the order of 10^{-4} . The retained terms in the equations of disturbance motion, e.g., $M_u^+ \delta u^+$, are of the order of 10^{-1} . It is clear that neglecting terms like $\hat{\omega}_{bd} \times \hat{v}_{cg}$ is reasonable.

3.3.3 The mean inertial force and moment of the flapping wings being approximately zero

Recall that in Sect. 2.3, \bar{b}_1 and \bar{b}_2 in Eqs. (18) and (19), which represent the mean inertial forces and moments of the flapping wings, were dropped on the assumption that they were approximately zero. This is checked here. To compute \bar{b}_1 and \bar{b}_2 , we need ω_{wg0} , ω_{bd} and v_{cg} (see Eqs. 13 and 15). ω_{wg0} is known because the flapping motions is prescribed. ω_{bd} and v_{cg} can be estimated on the basis of the natural modes of motion of the body. Thus, \bar{b}_1 and \bar{b}_2 can be estimated. Our calculations show that the contributions of \bar{b}_1 and \bar{b}_2 to the equations of disturbance motion are approximately zero (the values of which are the order of 10^{-6}). The reason for this is because there are acceleration and deceleration of the wing within a down- or upstroke and the motion of the wing in the downstroke is opposite to that of the upstroke, the inertial forces (or moments) in deferent parts of a flapping cycle approximately cancel out (this was anticipated above).

The above analysis show that for insects, with relatively high wingbeat frequency (hoverfly, dronefly, bumblebee; n larger than 150 Hz), the “rigid body” assumption and the simplification of the equations of motion are reasonable, but for insects with relatively small wingbeat frequency (cranefly and hawkmoth; n less than 45 Hz), because the requirement of body motion being much slower than wing flapping motion is not well met, the applicability of the “rigid body” assumption is questionable.

Table 7 Approximate eigenvalues for insects in normal hovering computed by Eqs. (31), (34)–(38)

	Mode 1 $\lambda_{1,2}$	Mode 2 λ_3	Mode 3 λ_4
HF	0.010±0.019i	−0.023	−0.003
DF	0.010±0.019i	−0.023	−0.002
CF	0.025±0.052i	−0.065	−0.008
HM	0.044±0.095i	−0.120	−0.015

3.4 Approximate analytical expressions of the eigenvalues and physical interpretation of the natural modes

In order to have physical insight into the genesis of the natural modes of motion, it is desirable to have approximate analytical expressions for the eigenvalues. Here, we obtain the expressions by simplifying the equations of motion on the basis of the known modal characteristics.

First, we consider the stable slow subsidence mode. We have noted that δu , δq and $\delta \theta$ are negligibly small in this mode (Table 5, mode 3). We can therefore simplify the equations of motion (Eq. 27) by neglecting the X -force equation, the pitching moment equation and the $\delta \theta$ -equation and putting δu , δq and $\delta \theta$ to zero in the Z -force equation. This results in the simplified equation:

$$\delta \dot{w}^+ = \frac{Z_w^+}{m_{bd}^+} \delta w^+. \tag{29}$$

The characteristic equation is

$$\lambda - Z_w^+ / m_{bd}^+ = 0, \tag{30}$$

which gives the approximate expression for the eigenvalue of the stable slow subsidence mode (λ_4) as

$$\lambda_4 \approx Z_w^+ / m_{bd}^+. \tag{31}$$

Values of λ_4 computed by Eq. (31) are given in Table 7 and they are almost identical to the exact values shown in Table 4 (λ_4 for the bumblebee studied by Sun and Xiong [7] computed by Eq. (31) is -1.795 , almost the same as the exact value -1.799). From Eq. (31), we see that the stable slow subsidence mode mainly depends on the ratio of two parameters, Z_w and m_{bd} . The physical interpretation of this mode of motion is clearly seen: when Z_w is negative, for example, a positive Δw disturbance (insect moving downward) will produce a negative vertical force, which opposes the downward motion, stabilizing the motion.

Next, we consider the unstable oscillatory mode and the stable fast subsidence mode. In these two modes (Table 5, modes 1 and 2), δw is negligibly small. Therefore, we can neglect the Z -force equation and set δw in other equations zero. The equations of motion (Eq. 27) are simplified to the

following:

$$\begin{bmatrix} \delta \dot{u}^+ \\ \delta \dot{q}^+ \\ \delta \dot{\theta}^+ \end{bmatrix} = \begin{bmatrix} X_u^+ / m_{bd}^+ & X_u^+ / m_{bd}^+ & -g^+ \\ M_u^+ / I_y^+ & M_q^+ / I_y^+ & 0 \\ 0 & 1 & 0 \end{bmatrix} \begin{bmatrix} \delta u^+ \\ \delta q^+ \\ \delta \theta^+ \end{bmatrix}. \tag{32}$$

The characteristic equation of which is

$$\lambda^3 - \left(\frac{X_u^+}{m_{bd}^+} + \frac{M_q^+}{I_y^+} \right) \lambda^2 + \left(\frac{X_u^+ M_q^+}{m_{bd}^+ I_y^+} - \frac{M_u^+ X_q^+}{m_{bd}^+ I_y^+} \right) \lambda + \frac{g^+ M_u^+}{I_y^+} = 0. \tag{33}$$

The exact expressions of the roots of Eq. (33) can be obtained. But the expressions are rather complex and it is difficult to see how a parameter influences the roots. By using the binomial series expansion and neglecting the higher order terms, we obtain relatively simple expressions of the roots (see the Appendix B):

$$\lambda_{1,2} = \hat{n} \pm i \hat{\omega}, \tag{34}$$

where

$$\hat{n} \approx \frac{1}{2} \sqrt[3]{\frac{M_u^+ g^+}{I_y^+}} (1 - 2j), \tag{35}$$

$$\hat{\omega} \approx \frac{\sqrt{3}}{2} \sqrt[3]{\frac{M_u^+ g^+}{I_y^+}}, \tag{36}$$

and

$$\lambda_3 \approx -\sqrt[3]{\frac{M_u^+ g^+}{I_y^+}} (1 + j), \tag{37}$$

where

$$j = -\frac{1}{3} \left(\frac{M_q^+}{I_y^+} + \frac{X_u^+}{m_{bd}^+} \right) / \sqrt[3]{\frac{M_u^+ g^+}{I_y^+}}. \tag{38}$$

Values of $\lambda_{1,2}$ and λ_3 computed using Eqs. (34)–(38) are also given in Table 7, which are in very good agreement with the exact values given in Table 4 (this is also true for the bumblebee studied by Sun and Xiong [7]).

Using data in Tables 1 and 3, it can be shown that j is considerably smaller than 1. We thus see that $\sqrt[3]{M_u^+ g^+ / I_y^+}$ plays a major role in determining $\lambda_{1,2}$ ($= \hat{n} \pm i \hat{\omega}$) and λ_3 ; i.e., these two modes are mainly determined by the parameters M_u , g and I_y . On the basis of these results, the physical interpretation of the two natural modes of motion can be given. For the unstable oscillatory mode, when the insect moves forward (positive Δu), it pitches up (as seen above, u and q are approximately in phase); the positive Δu produces a positive moment $M_u \Delta u$, which tends to increase the pitch-up motion, destabilizing the motion (similar destabilizing effects can be seen when the insect moves backwards). For the fast subsidence mode, the opposite is true: when the insect moves forward, it pitches down (as seen above, u and q are

approximately out of phase); the positive moment produced by Δu tends to decrease the pitch-down motion, stabilizing the motion (similar stabilizing effects can be seen when the insect moves backwards).

4 Conclusions

1. For insects considered in the present study and in Ref. [7], for those with relatively high wingbeat frequency (hoverfly, drone fly and bumblebee), the “rigid body” assumption is reasonable, and for those with relatively low wingbeat frequency (crane fly and howkmoth), the applicability of the “rigid body” assumption is questionable.
2. The same three natural modes of motion as those reported recently for a bumblebee are identified, i.e., one unstable oscillatory mode, one stable fast subsidence mode and one stable slow subsidence mode.
3. Approximate analytical expressions of the eigenvalues, which give physical insight into the genesis of the natural modes of motion, are derived. The expressions identify the speed derivative M_u (pitching moment produced by unit horizontal speed) as the primary source of the unstable oscillatory mode and the stable fast subsidence mode and Z_w (vertical force produced by unit vertical speed) as the primary source of the stable slow subsidence mode.

Appendix A Derivation of the equations of motion

A.1 Translational equations of the motion

Variables v_{cg} , ω_{bd} , R_{cg} , R_h , R_{wg} , etc. have been defined in the text. Newton’s law is applied to an element dm of the insect and then integrated over all elements. The position vector of dm relative to the origin of the inertial frame is $R_{cg} + R$, where R is a vector from the centre of mass of the body to dm . The inertial velocity of dm is

$${}_f v = \frac{d}{dt}({}_f R_{cg} + {}_f R) = {}_f v_{cg} + \frac{d_f R}{dt}. \tag{A1}$$

The momentum of dm is $v dm$, and of the whole insect is:

$$\begin{aligned} \int_{\text{body \& wings}} {}_f v dm &= \int_{\text{body \& wings}} \left({}_f v_{cg} + \frac{d_f R}{dt} \right) dm \\ &= m_{\text{total}} {}_f v_{cg} + \int_{\text{body \& wings}} \frac{d_f R}{dt} dm \end{aligned} \tag{A2}$$

where m_{total} is the total mass of the body and wings of the insect. Newton’s second law applied to dm gives:

$$d_f f = \frac{d_f v}{dt} dm, \tag{A3}$$

where $d_f f$ is the force acting on the element. Integration over the insect gives:

$$\begin{aligned} {}_f F &= m_{\text{total}} \frac{d_f v_{cg}}{dt} + \int_{\text{body \& wings}} \frac{d^2_f R}{dt^2} dm \\ &= m_{\text{total}} \frac{d_f v_{cg}}{dt} + \frac{d^2}{dt^2} \int_{\text{body}} {}_f R dm + \sum_{i=1}^N \frac{d^2}{dt^2} \int_{\text{wing},i} {}_f R dm, \end{aligned} \tag{A4}$$

where F is the force acting on the insect and N is the number of wings. Since R is a vector from the centre of mass of the body, we have:

$$\int_{\text{body}} {}_f R dm = 0. \tag{A5}$$

For a point on a wing (Fig. 1),

$${}_f R = {}_f R_h + {}_f R_{wg} + {}_f R_p, \tag{A6}$$

where R_p is a vector from the centre of mass of the wing. Since $(R_h + R_{wg})$ is constant in the integration, we have:

$$\begin{aligned} \int_{\text{wing}} {}_f R dm &= \int_{\text{wing}} ({}_f R_h + {}_f R_{wg} + {}_f R_p) dm \\ &= m_{wg} ({}_f R_h + {}_f R_{wg}), \end{aligned} \tag{A7}$$

where m_{wg} is the mass of the wing. Substituting Eqs. (A5) and (A7) into Eq. (A4) gives:

$${}_f F = m_{\text{total}} \frac{d_f v_{cg}}{dt} + \sum_{i=1}^N m_{wg,i} \frac{d^2}{dt^2} ({}_f R_h + {}_f R_{wg})_i. \tag{A8}$$

Equation (A8) is in the inertial frame. As will be seen below, in deriving the rotational equation of motion, time derivatives of angular momentum, which contains moments and products of inertia of the body, are needed. If equations of motion are written in body frame, moments and products of inertia of the body would be independent on time and the resulting equations would be relatively simple. Therefore, it is desirable to rewrite the equations of motion in the body frame (x_b, y_b, z_b) . Equation (A8) can be transformed to frame (x_b, y_b, z_b) by using the following relations [13]:

$$\frac{d_f V}{dt} = \frac{d_b V}{dt} + {}_b \omega_{bd} \times {}_b V, \tag{A9}$$

$$\begin{aligned} \frac{d^2_f V}{dt^2} &= \frac{d^2_b V}{dt^2} + 2{}_b \omega_{bd} \times \frac{d_b V}{dt} + \frac{d_b \omega_{bd}}{dt} \times {}_b V \\ &\quad + {}_b \omega_{bd} \times ({}_b \omega_{bd} \times {}_b V). \end{aligned} \tag{A10}$$

When ${}_b\mathbf{V}$ and ${}_b\boldsymbol{\omega}_{bd}$ are changed to ${}_w\mathbf{V}$ and ${}_w\boldsymbol{\omega}_{wg}$, respectively, Eqs. (A9) and (A10) relate the time derivatives of ${}_f\mathbf{V}$ and ${}_w\mathbf{V}$. Applying these relations to the terms on the right hand side (RHS) of Eq. (A8) gives:

$$\frac{d{}_f\mathbf{v}_{cg}}{dt} = \frac{d{}_b\mathbf{v}_{cg}}{dt} + {}_b\boldsymbol{\omega}_{bd} \times {}_b\mathbf{v}_{cg}, \tag{A11}$$

$$\frac{d^2{}_f\mathbf{R}_h}{dt^2} = \frac{d{}_b\boldsymbol{\omega}_{bd}}{dt} \times {}_b\mathbf{R}_h + {}_b\boldsymbol{\omega}_{bd} \times ({}_b\boldsymbol{\omega}_{bd} \times {}_b\mathbf{R}_h), \tag{A12}$$

$$\frac{d^2{}_f\mathbf{R}_{wg}}{dt^2} = \frac{d{}_w\boldsymbol{\omega}_{wg}}{dt} \times {}_w\mathbf{R}_{wg} + {}_w\boldsymbol{\omega}_{wg} \times ({}_w\boldsymbol{\omega}_{wg} \times {}_w\mathbf{R}_{wg}). \tag{A13}$$

Thus Eq. (A8) can be rewritten as

$$\begin{aligned} {}_b\mathbf{F} = m_{total} & \left(\frac{d{}_b\mathbf{v}_{cg}}{dt} + {}_b\boldsymbol{\omega}_{bd} \times {}_b\mathbf{v}_{cg} \right) + \sum_{i=1}^N \left\{ m_{wg} \left[\frac{d{}_b\boldsymbol{\omega}_{bd}}{dt} \right. \right. \\ & \left. \left. \times {}_b\mathbf{R}_h + {}_b\boldsymbol{\omega}_{bd} \times ({}_b\boldsymbol{\omega}_{bd} \times {}_b\mathbf{R}_h) \right] \right\}_i + \sum_{i=1}^N \left\{ m_{wg} \frac{\mathbf{E}}{w \rightarrow b} \right. \\ & \left. \times \left[\frac{d{}_w\boldsymbol{\omega}_{wg}}{dt} \times {}_w\mathbf{R}_{wg} + {}_w\boldsymbol{\omega}_{wg} \times ({}_w\boldsymbol{\omega}_{wg} \times {}_w\mathbf{R}_{wg}) \right] \right\}_i, \end{aligned} \tag{A14}$$

which is the translational equation of motion.

A.2 Rotational equations of motion

The moment of momentum of dm with respect to the origin of the inertial frame is

$$d{}_f\mathbf{H} = {}_f\mathbf{R}_1 \times {}_f\mathbf{v}dm, \tag{A15}$$

where \mathbf{R}_1 is a vector from the origin of the inertial frame, Newton’s second law written for the angular momentum gives:

$$d{}_f\mathbf{M}_1 = \frac{d}{dt}(d{}_f\mathbf{H}) = \frac{d}{dt}({}_f\mathbf{R}_1 \times {}_f\mathbf{v}dm), \tag{A16}$$

where $d{}_f\mathbf{M}_1$ is the moment acting on the element about the origin of the inertial frame. Integrating over the insect gives:

$${}_f\mathbf{M}_1 = \frac{d{}_f\mathbf{H}}{dt}, \tag{A17}$$

where \mathbf{M}_1 is the moment acting on the insect about the origin of the inertial frame and \mathbf{H} can be written as follows:

$$\begin{aligned} {}_f\mathbf{H} &= \int_{\text{body \& wings}} {}_f\mathbf{R}_1 \times {}_f\mathbf{v}dm \\ &= \int_{\text{body}} {}_f\mathbf{R}_1 \times {}_f\mathbf{v}dm + \sum_{i=1}^N \int_{\text{wing},i} {}_f\mathbf{R}_1 \times {}_f\mathbf{v}dm. \end{aligned} \tag{A18}$$

At a point on the body, inertial velocity is

$${}_f\mathbf{v} = \frac{d}{dt}({}_f\mathbf{R}_{cg} + {}_f\mathbf{R}) = {}_f\mathbf{v}_{cg} + {}_f\boldsymbol{\omega}_{bd} \times {}_f\mathbf{R}. \tag{A19}$$

At a point on a wing (\mathbf{R} is $\mathbf{R}_h + \mathbf{R}_{wg} + \mathbf{R}_p$), inertial velocity is

$$\begin{aligned} {}_f\mathbf{v} &= \frac{d}{dt}({}_f\mathbf{R}_{cg} + {}_f\mathbf{R}_h + {}_f\mathbf{R}_{wg} + {}_f\mathbf{R}_p) \\ &= \frac{d}{dt}({}_f\mathbf{R}_{cg} + {}_f\mathbf{R}_h) + {}_f\boldsymbol{\omega}_{wg} \times ({}_f\mathbf{R}_{wg} + {}_f\mathbf{R}_p) \\ &= {}_f\mathbf{v}_{cg} + {}_f\boldsymbol{\omega}_{bd} \times {}_f\mathbf{R}_h + {}_f\boldsymbol{\omega}_{wg} \times ({}_f\mathbf{R}_{wg} + {}_f\mathbf{R}_p). \end{aligned} \tag{A20}$$

\mathbf{R}_1 can be written as

$${}_f\mathbf{R}_1 = {}_f\mathbf{R}_{cg} + {}_f\mathbf{R} \quad (\text{for point on body}), \tag{A21}$$

$${}_f\mathbf{R}_1 = {}_f\mathbf{R}_{cg} + {}_f\mathbf{R}_h + {}_f\mathbf{R}_{wg} + {}_f\mathbf{R}_p \quad (\text{for point on wing}). \tag{A22}$$

Using Eqs. (A19)–(A22), Eq. (A18) can be written as

$$\begin{aligned} {}_f\mathbf{H} &= \int_{\text{body}} ({}_f\mathbf{R}_{cg} + {}_f\mathbf{R}) \times {}_f\mathbf{v}_{cg}dm + \int_{\text{body}} ({}_f\mathbf{R}_{cg} + {}_f\mathbf{R}) \\ & \times ({}_f\boldsymbol{\omega}_{bd} \times {}_f\mathbf{R})dm + \sum_{i=1}^N \int_{\text{wing},i} ({}_f\mathbf{R}_{cg} + {}_f\mathbf{R}_h + {}_f\mathbf{R}_{wg} \\ & + {}_f\mathbf{R}_p) \times ({}_f\mathbf{v}_{cg} + {}_f\boldsymbol{\omega}_{bd} \times {}_f\mathbf{R}_h)dm + \sum_{i=1}^N \int_{\text{wing},i} ({}_f\mathbf{R}_{cg} \\ & + {}_f\mathbf{R}_h + {}_f\mathbf{R}_{wg} + {}_f\mathbf{R}_p) \times [{}_f\boldsymbol{\omega}_{wg} \times ({}_f\mathbf{R}_{wg} + {}_f\mathbf{R}_p)]dm. \end{aligned} \tag{A23}$$

The terms on the RHS of Eq. (A23) can be simplified as following. The first term becomes:

$$\begin{aligned} & \int_{\text{body}} {}_f\mathbf{R}_{cg} \times {}_f\mathbf{v}_{cg}dm + \int_{\text{body}} {}_f\mathbf{R} \times {}_f\mathbf{v}_{cg}dm \\ &= m_{bdf} \mathbf{R}_{cg} \times {}_f\mathbf{v}_{cg}, \end{aligned} \tag{A24}$$

where m_{bd} is the mass of the body and the second integration is zero because \mathbf{R} is a vector from the centre of mass of the body. The second term on the RHS of Eq. (A23) becomes:

$$\begin{aligned} & \int_{\text{body}} {}_f\mathbf{R}_{cg} \times ({}_f\boldsymbol{\omega}_{bd} \times {}_f\mathbf{R})dm + \int_{\text{body}} {}_f\mathbf{R} \times ({}_f\boldsymbol{\omega}_{bd} \times {}_f\mathbf{R})dm \\ &= \int_{\text{body}} {}_f\mathbf{R} \times ({}_f\boldsymbol{\omega}_{bd} \times {}_f\mathbf{R})dm = {}_f\mathbf{I}_{bdf} \boldsymbol{\omega}_{bd}, \end{aligned} \tag{A25}$$

where I_{bd} is the inertia matrix of the body. The third term on the RHS of Eq. (A23) becomes:

$$\sum_{i=1}^N \int_{\text{wing},i} (fR_{cg} + fR_h + fR_{wg} + fR_p) \times (fv_{cg} + f\omega_{bd} \times fR_h) dm = \sum_{i=1}^N [m_{wg}(fR_{cg} + fR_h + fR_{wg}) \times (fv_{cg} + f\omega_{bd} \times fR_h)]_i, \tag{A26}$$

because in the integration, $(R_{cg} + R_h + R_{wg})$ and $(fv_{cg} + f\omega_{bd} \times fR_h)$ are constant and R_p is a vector from the centre of mass of the wing. The fourth term on the RHS of Eq. (A23) becomes:

$$\sum_{i=1}^N \int_{\text{wing},i} (fR_{cg} + fR_h + fR_{wg} + fR_p) \times [f\omega_{wg} \times (fR_{wg} + fR_p)] dm = \sum_{i=1}^N \{m_{wg}(fR_{cg} + fR_h) \times (f\omega_{wg} \times fR_{wg}) + \int_{\text{wing}} (fR_{wg} + fR_p) \times [f\omega_{wg} \times (fR_{wg} + fR_p)] dm\}_i = \sum_{i=1}^N [m_{wg}(fR_{cg} + fR_h) \times (f\omega_{wg} \times fR_{wg}) + fI_{wg}f\omega_{wg}]_i, \tag{A27}$$

where

$$fI_{wg}f\omega_{wg} = \int_{\text{wing}} (fR_{wg} + fR_p) \times [f\omega_{wg} \times (fR_{wg} + fR_p)] dm, \tag{A28}$$

and I_{wg} is the inertia matrix of the wing. Substituting Eqs. (A24)–(A27) into Eq. (A23), fH is written as

$$fH = m_{bdf}R_{cg} \times fv_{cg} + fI_{bdf}\omega_{bd} + \sum_{i=1}^N [m_{wgf}R_{cg} \times (fv_{cg} + f\omega_{bd} \times fR_h) + m_{wgf}R_{cg} \times (f\omega_{wg} \times fR_{wg})]_i + \sum_{i=1}^N [m_{wg}(fR_h + fR_{wg}) \times (fv_{cg} + f\omega_{bd} \times fR_h) + m_{wgf}R_h \times (f\omega_{wg} \times fR_{wg}) + fI_{wg}f\omega_{wg}]_i. \tag{A29}$$

The time rate of change of fH is

$$\begin{aligned} \frac{d_f H}{dt} &= m_{bdf}R_{cg} \times \frac{d_f v_{cg}}{dt} + m_{bd} \frac{d_f R_{cg}}{dt} \times f v_{cg} \\ &+ \sum_{i=1}^N \left[m_{wg} \frac{d_f R_{cg}}{dt} \times (f v_{cg} + f \omega_{bd} \times f R_h) \right. \\ &+ m_{wgf} R_{cg} \times \frac{d_f v_{cg}}{dt} + m_{wgf} R_{cg} \times \frac{d}{dt} (f \omega_{bd} \times f R_h) \left. \right]_i \\ &+ \sum_{i=1}^N \left[m_{wg} \frac{d_f R_{cg}}{dt} \times (f \omega_{wg} \times f R_{wg}) \right. \\ &+ m_{wgf} R_{cg} \times \frac{d}{dt} (f \omega_{wg} \times f R_{wg}) \left. \right]_i + \frac{d}{dt} (f I_{bdf} \omega_{bd}) \\ &+ \sum_{i=1}^N \frac{d}{dt} [m_{wg}(f R_h + f R_{wg}) \times (f v_{cg} + f \omega_{bd} \times f R_h) \\ &+ m_{wgf} R_h \times (f \omega_{wg} \times f R_{wg}) + f I_{wg} f \omega_{wg}]_i \\ &= m_{bdf}R_{cg} \times \frac{d_f v_{cg}}{dt} + \sum_{i=1}^N \left[m_{wgf} v_{cg} \times (f \omega_{bd} \times f R_h) \right. \\ &+ m_{wgf} R_{cg} \times \frac{d_f v_{cg}}{dt} + m_{wgf} R_{cg} \times \frac{d}{dt} (f \omega_{bd} \times f R_h) \left. \right]_i \\ &+ \sum_{i=1}^N \left[m_{wgf} v_{cg} \times (f \omega_{wg} \times f R_{wg}) \right. \\ &+ m_{wgf} R_{cg} \times \frac{d}{dt} (f \omega_{wg} \times f R_{wg}) \left. \right]_i \\ &+ \frac{d}{dt} (f I_{bdf} \omega_{bd}) + \sum_{i=1}^N \frac{d}{dt} [m_{wg}(f R_h + f R_{wg}) \\ &\times (f v_{cg} + f \omega_{bd} \times f R_h) \\ &+ m_{wgf} R_h \times (f \omega_{wg} \times f R_{wg}) + f I_{wg} f \omega_{wg}]_i. \tag{A30} \end{aligned}$$

M_1 in Eq. (A17) (the moment acting on the insect) is about the origin of the inertial frame. It can be written as

$$fM_1 = fM + fR_{cg} \times fF, \tag{A31}$$

where M is the moment acting on the insect about the center of mass of the body and F is the force acting on the insect. Using Eq. (A8), (A31) becomes

$$\begin{aligned} fM_1 &= fM + fR_{cg} \times \left[m_{total} \frac{d_f v_{cg}}{dt} \right. \\ &+ \left. \sum_{i=1}^N m_{wg,i} \frac{d^2}{dt^2} (fR_h + fR_{wg})_i \right] \\ &= fM + m_{total} fR_{cg} \times \frac{d_f v_{cg}}{dt} \\ &+ \sum_{i=1}^N \left[m_{wgf} R_{cg} \times \frac{d^2}{dt^2} (fR_h + fR_{wg}) \right]_i \\ &= fM + m_{total} fR_{cg} \times \frac{d_f v_{cg}}{dt} \end{aligned}$$

$$\begin{aligned}
 & + \sum_{i=1}^N \left[m_{wgf} \mathbf{R}_{cg} \times \frac{d}{dt} (\mathbf{f}\boldsymbol{\omega}_{bd} \times \mathbf{f}\mathbf{R}_h + \mathbf{f}\boldsymbol{\omega}_{wg} \times \mathbf{f}\mathbf{R}_{wg}) \right]_i \\
 = & \mathbf{f}\mathbf{M} + m_{totalf} \mathbf{R}_{cg} \times \frac{d\mathbf{f}\mathbf{v}_{cg}}{dt} \\
 & + \sum_{i=1}^N \left[m_{wgf} \mathbf{R}_{cg} \times \frac{d}{dt} (\mathbf{f}\boldsymbol{\omega}_{bd} \times \mathbf{f}\mathbf{R}_h) \right]_i \\
 & + \sum_{i=1}^N \left[m_{wgf} \mathbf{R}_{cg} \times \frac{d}{dt} (\mathbf{f}\boldsymbol{\omega}_{wg} \times \mathbf{f}\mathbf{R}_{wg}) \right]_i. \tag{A32}
 \end{aligned}$$

Substituting Eqs. (A30) and (A32) into Eq. (A17) and noting that

$$m_{bd} + \sum_{i=1}^N m_{wg,i} = m_{total}, \tag{A33}$$

Eq. (A17) becomes

$$\begin{aligned}
 \mathbf{f}\mathbf{M} = & \sum_{i=1}^N [m_{wgf} \mathbf{v}_{cg} \times (\mathbf{f}\boldsymbol{\omega}_{bd} \times \mathbf{f}\mathbf{R}_h + \mathbf{f}\boldsymbol{\omega}_{wg} \times \mathbf{f}\mathbf{R}_{wg})]_i \\
 & + \frac{d}{dt} (\mathbf{f}\mathbf{I}_{bdf} \boldsymbol{\omega}_{bd}) + \sum_{i=1}^N \frac{d}{dt} [m_{wg} (\mathbf{f}\mathbf{R}_h + \mathbf{f}\mathbf{R}_{wg}) \\
 & \times (\mathbf{f}\mathbf{v}_{cg} + \mathbf{f}\boldsymbol{\omega}_{bd} \times \mathbf{f}\mathbf{R}_h) + m_{wgf} \mathbf{R}_h \\
 & \times (\mathbf{f}\boldsymbol{\omega}_{wg} \times \mathbf{f}\mathbf{R}_{wg}) + \mathbf{f}\mathbf{I}_{wgf} \boldsymbol{\omega}_{wg}]_i. \tag{A34}
 \end{aligned}$$

Equation (A34) is the rotational equation of motion in inertial frame. It is transformed into the body frame using Eqs. (A9) and (A10). First, the time derivative terms on the RHS are treated separately as following:

$$\frac{d}{dt} (\mathbf{f}\mathbf{I}_{bdf} \boldsymbol{\omega}_{bd}) = \frac{d}{dt} (\mathbf{b}\mathbf{I}_{bdb} \boldsymbol{\omega}_{bd}) + \mathbf{b}\boldsymbol{\omega}_{bd} \times \mathbf{b}\mathbf{I}_{bdb} \boldsymbol{\omega}_{bd}, \tag{A35}$$

$$\begin{aligned}
 & \frac{d}{dt} [(\mathbf{f}\mathbf{R}_h + \mathbf{f}\mathbf{R}_{wg}) \times (\mathbf{f}\mathbf{v}_{cg} + \mathbf{f}\boldsymbol{\omega}_{bd} \times \mathbf{f}\mathbf{R}_h)] \\
 = & \frac{d}{dt} [(\mathbf{b}\mathbf{R}_h + \mathbf{b}\mathbf{R}_{wg}) \times (\mathbf{b}\mathbf{v}_{cg} + \mathbf{b}\boldsymbol{\omega}_{bd} \times \mathbf{b}\mathbf{R}_h)] \\
 & + \mathbf{b}\boldsymbol{\omega}_{bd} \times [(\mathbf{b}\mathbf{R}_h + \mathbf{b}\mathbf{R}_{wg}) \times (\mathbf{b}\mathbf{v}_{cg} + \mathbf{b}\boldsymbol{\omega}_{bd} \times \mathbf{b}\mathbf{R}_h)], \tag{A36}
 \end{aligned}$$

$$\begin{aligned}
 & \frac{d}{dt} [\mathbf{f}\mathbf{R}_h \times (\mathbf{f}\boldsymbol{\omega}_{wg} \times \mathbf{f}\mathbf{R}_{wg})] \\
 = & \frac{d}{dt} [\mathbf{b}\mathbf{R}_h \times (\mathbf{b}\boldsymbol{\omega}_{wg} \times \mathbf{b}\mathbf{R}_{wg})] + \mathbf{b}\boldsymbol{\omega}_{bd} \\
 & \times [\mathbf{b}\mathbf{R}_h \times (\mathbf{b}\boldsymbol{\omega}_{wg} \times \mathbf{b}\mathbf{R}_{wg})], \tag{A37}
 \end{aligned}$$

$$\begin{aligned}
 \frac{d}{dt} (\mathbf{f}\mathbf{I}_{wgf} \boldsymbol{\omega}_{wg}) = & \frac{d}{dt} (\mathbf{b}\mathbf{I}_{wgb} \boldsymbol{\omega}_{wg}) + \mathbf{b}\boldsymbol{\omega}_{bd} \times \mathbf{b}\mathbf{I}_{wgb} \boldsymbol{\omega}_{wg} \\
 = & \frac{d}{dt} [\mathbf{E}_{w \rightarrow b} (\mathbf{w}\mathbf{I}_{wgw} \boldsymbol{\omega}_{wg})] \\
 & + \mathbf{b}\boldsymbol{\omega}_{bd} \times \mathbf{E}_{w \rightarrow b} (\mathbf{w}\mathbf{I}_{wgw} \boldsymbol{\omega}_{wg}). \tag{A38}
 \end{aligned}$$

Using Eqs. (A35)–(A38), Eq. (A34) is transformed into the body frame as following:

$$\begin{aligned}
 \mathbf{b}\mathbf{M} = & \sum_{i=1}^N [m_{wgb} \mathbf{v}_{cg} \times (\mathbf{b}\boldsymbol{\omega}_{bd} \times \mathbf{b}\mathbf{R}_h + \mathbf{b}\boldsymbol{\omega}_{wg} \times \mathbf{b}\mathbf{R}_{wg})]_i \\
 & + \mathbf{b}\boldsymbol{\omega}_{bd} \times \mathbf{b}\mathbf{I}_{bdb} \boldsymbol{\omega}_{bd} + \frac{d}{dt} \{ \mathbf{b}\mathbf{I}_{bdb} \boldsymbol{\omega}_{bd} \\
 & + \sum_{i=1}^N [m_{wg} (\mathbf{b}\mathbf{R}_h + \mathbf{b}\mathbf{R}_{wg}) \times (\mathbf{b}\mathbf{v}_{cg} + \mathbf{b}\boldsymbol{\omega}_{bd} \times \mathbf{b}\mathbf{R}_h) \\
 & + m_{wgb} \mathbf{R}_h \times (\mathbf{b}\boldsymbol{\omega}_{wg} \times \mathbf{b}\mathbf{R}_{wg}) + \mathbf{E}_{w \rightarrow b} (\mathbf{w}\mathbf{I}_{wgw} \boldsymbol{\omega}_{wg})]_i \} \\
 & + \sum_{i=1}^N \{ \mathbf{b}\boldsymbol{\omega}_{bd} \times \mathbf{E}_{w \rightarrow b} (\mathbf{w}\mathbf{I}_{wgw} \boldsymbol{\omega}_{wg}) + m_{wgb} \boldsymbol{\omega}_{bd} \\
 & \times [\mathbf{b}\mathbf{R}_h \times (\mathbf{b}\boldsymbol{\omega}_{wg} \times \mathbf{b}\mathbf{R}_{wg})] + m_{wgb} \boldsymbol{\omega}_{bd} \\
 & \times [(\mathbf{b}\mathbf{R}_h + \mathbf{b}\mathbf{R}_{wg}) \times (\mathbf{b}\mathbf{v}_{cg} + \mathbf{b}\boldsymbol{\omega}_{bd} \times \mathbf{b}\mathbf{R}_h)] \}_i. \tag{A39}
 \end{aligned}$$

Equation (A39) is the rotational equation of motion in body frame.

Appendix B Derivation of approximate roots

Letting $b = -\left(\frac{X_u^+}{m_{bd}^+} + \frac{M_q^+}{I_y^+}\right)$, $c = \left(\frac{X_u^+ M_q^+}{m_{bd}^+ I_y^+} - \frac{M_u^+ X_q^+}{m_{bd}^+ I_y^+}\right)$ and $d = \frac{g^+ M_u^+}{I_y^+}$, Eq. (A33) can be written as

$$\lambda^3 + b\lambda^2 + c\lambda + d = 0. \tag{B1}$$

From the values of M_u^+ , M_q^+ , etc. (Table 3), we have $b > 0$, $c > 0$ and $d > 0$. Letting

$$p = c - b^2/3, \tag{B2}$$

$$q = 2b^3/27 + d - bc/3, \tag{B3}$$

the roots of Eq. (B1) are [14]:

$$\lambda_{1,2} = \hat{n} \pm i\hat{\omega}, \tag{B4}$$

where

$$\hat{n} = -\frac{1}{2} \left(\sqrt[3]{-A+B} + \sqrt[3]{-A-B} \right) - \frac{b}{3}, \tag{B5}$$

$$\hat{\omega} = \frac{\sqrt{3}}{2} \left(\sqrt[3]{-A+B} - \sqrt[3]{-A-B} \right), \tag{B6}$$

and

$$\lambda_3 = \sqrt[3]{-A+B} + \sqrt[3]{-A-B} - \frac{b}{3}. \tag{B7}$$

A and B in the above equations are defined as

$$A = \frac{q}{2} = \frac{d}{2} (1 + \alpha - \beta), \tag{B8}$$

$$B = \sqrt{\frac{q^2}{4} + \frac{p^3}{27}} = \frac{d}{2} \left(1 + 2\alpha - 2\beta + \frac{1}{3}\beta^2 + \gamma \right)^{1/2}, \tag{B9}$$

where $\alpha = (b/3)^3 \cdot (2/d)$, $\beta = (b/3) \cdot (c/d)$, $\gamma = (4/27) \cdot (c/d)^2 \cdot c$.

Using the values of m , I_y , M_u etc. in Tables 1 and 3, it can be shown that α and β are generally much smaller than 1 and that γ is the same order of magnitude as β^2 . Thus, approximate, but simple, expressions for $\lambda_{1,2}$ and λ_3 can be obtained using the binomial series expansion with the higher order terms (HOT) dropped. This is done as follows:

$$\begin{aligned} \sqrt[3]{-A+B} &= \left[-\frac{d}{2}(1+\alpha-\beta) + \frac{d}{2}\left(1+\alpha-\beta - \frac{1}{2}\alpha^2 - \frac{2}{3}\beta^2 + \alpha\beta + \frac{1}{2}\gamma + \text{HOT}\right) \right]^{1/3} \\ &\approx -\sqrt[3]{d} \sqrt[3]{\frac{\alpha^2}{4} + \frac{\beta^2}{3} - \frac{\alpha\beta}{2} - \frac{\gamma}{4}}, \end{aligned} \tag{B10}$$

$$\begin{aligned} \sqrt[3]{-A-B} &= \left[-\frac{d}{2}(1+\alpha-\beta) - \frac{d}{2}(1+\alpha-\beta + \text{HOT}) \right]^{1/3} \\ &\approx -\sqrt[3]{d} \left(1 + \frac{1}{3}\alpha - \frac{1}{3}\beta \right) \approx -\sqrt[3]{d}. \end{aligned} \tag{B11}$$

Using Eqs. (B10) and (B11), we have

$$-\frac{1}{2}(\sqrt[3]{-A+B} + \sqrt[3]{-A-B}) - \frac{b}{3} \approx \frac{1}{2}\sqrt[3]{d} \left(1 - 2\sqrt[3]{\frac{\alpha}{2}} \right), \tag{B12}$$

$$\frac{\sqrt{3}}{2}(\sqrt[3]{-A+B} + \sqrt[3]{-A-B}) \approx \frac{\sqrt{3}}{2}\sqrt[3]{d}, \tag{B13}$$

$$\sqrt[3]{-A+B} + \sqrt[3]{-A-B} - b/3 = -\sqrt[3]{d} \left(1 + \sqrt[3]{\frac{\alpha}{2}} \right). \tag{B14}$$

Finally the roots (Eqs. B4–B7) can be written as:

$$\lambda_{1,2} = \hat{n} \pm i\hat{\omega}, \tag{B15}$$

where

$$\hat{n} = \frac{1}{2}\sqrt[3]{d}(1-2j), \tag{B16}$$

$$\hat{\omega} = \frac{\sqrt{3}}{2}\sqrt[3]{d}, \tag{B17}$$

and

$$\lambda_3 = -\sqrt[3]{d}(1+j), \tag{B18}$$

where $j = \sqrt[3]{\frac{\alpha}{2}} = b/(3\sqrt[3]{d})$; in terms of I_y^+ , M_u^+ , etc., j is:

$$j = -\frac{1}{3} \left(\frac{M_q^+}{I_y^+} + \frac{X_u^+}{m_{bd}^+} \right) / \sqrt[3]{\frac{M_u^+ g^+}{I_y^+}}. \tag{B19}$$

References

1. Ellington, C.P., van den Berg, C., Willmott, A.P., Thomas, A.L.R.: Leading edge vortices in insect flight. *Nature* **347**, 472–473 (1996)
2. Dickinson, M.H., Lehman, F.O., Sane, S.P.: Wing rotation and the aerodynamic basis of insect flight. *Science* **284**, 1954–1960 (1999)
3. Sun, M., Tang, J.: Unsteady aerodynamic force generation by a model fruit fly wing in flapping motion. *J. Exp. Biol.* **205**, 55–70 (2002)
4. Thomas, A.L.R., Taylor, G.K.: Animal flight dynamics. I. Stability in gliding flight. *J. Theor. Biol.* **212**, 399–424 (2001)
5. Taylor, G.K., Thomas, A.L.R.: Animal flight dynamics. II. Longitudinal stability in flapping flight. *J. Theor. Biol.* **214**, 351–370 (2002)
6. Taylor, G.K., Thomas, A.L.R.: Dynamic flight stability in the desert locust *Schistocerca gregaria*. *J. Exp. Biol.* **206**, 2803–2829 (2003)
7. Sun, M., Xiong, Y.: Dynamic flight stability of a hovering bumblebee. *J. Exp. Biol.* **208**, 447–459 (2005)
8. Gebert, G., Gallmeier, P., Evers, J.: Equations of motion for flapping flight. *AIAA Paper*, pp 2002–4872 (2002)
9. Etkin, B., Reid, L.D.: *Dynamics of Flight: Stability and Control*. Wiley, New York (1996)
10. Ellington, C.P.: The aerodynamics of hovering insect flight. II. Morphological parameters. *Phil. Trans. R. Soc. Lond. B* **305**, 17–40 (1984)
11. Ellington, C.P.: The aerodynamics of hovering insect flight. III. Kinematics. *Phil. Trans. R. Soc. Lond. B* **305**, 79–113 (1984)
12. Ennos, A.R.: The kinematics and aerodynamics of the free flight of some diptera. *J. Exp. Biol.* **142**, 49–85 (1989)
13. Meriam, J.L.: *Dynamics*. Wiley, New York (1975)
14. Burington, R.S.: *Handbook of Mathematical Tables and Formulas*. McGraw-Hill, Inc. New York (1973)